# Quantized topological response in trapped quantum gases

Pengfei Zhang

*Department of Physics, Fudan University, Shanghai 200438, People's Republic of China*
*and Institute for Quantum Information and Matter & Walter Burke Institute for Theoretical Physics,*
*California Institute of Technology, Pasadena, California 91125, USA*

We study the quantized topological response of trapped one-dimensional quantum gases, which involves applying an optical pulse to a half-infinite region in an asymptotically harmonic trap and measuring the resulting density distribution. We prove that the corresponding linear response is described by a universal quantized formula in the thermodynamic limit, which is invariant under local continuous deformations of the trapping potential $V$, atom distribution $f_\Lambda$, the spatial envelope of the optical pulse $\Theta_p$, and the measurement region $\Theta_m$. Our numerical analysis confirms this prediction with high accuracy, and we show that a short but finite optical pulse duration only causes a violation of quantization near the transition time. Our work presents an exciting avenue for exploring quantized topological phenomena in trapped quantum gases.

*Introduction.* Understanding the phases of quantum many-body systems is one of the most important subjects in condensed matter physics. Nowadays, it has been realized that quantum systems are not only classified by their local order parameters [1], but also by their topological properties [2–12]. By definition, the topological properties of quantum systems are invariant under continuous deformations, and are thus much more stable against perturbations. In many cases, non-trivial quantum topology implies novel quantum responses, which can be directly measured in both solid-state materials [13–15] and quantum simulators [16–21]. As an example, without any symmetry constraint, band insulators in two dimensions (2D) can be classified by the Chern number of occupied bands [22,23]. A nonzero Chern number guarantees the existence of chiral edge states under the open boundary condition, which contribute to a quantized Hall conductance. Adding symmetry constraints further leads to the new concept of symmetry-protected topological phases, examples of which include the celebrated quantum spin Hall effect [24–26]. Unveiling new topological responses beyond the current knowledge is then of special interest.

Recently, Kane proposed that the topology of the Fermi surface can be probed by a novel quantized nonlinear charge transport in $D$ dimensions with $D \geqslant 2$ [27], which is a generalization of the Landauer formula in one dimension (1D) [28–36]. Studies further show that this Fermi-surface topology can also be probed using the entanglement entropy [37]. Later, a concrete experimental protocol for observing such quantized nonlinear transport was proposed in a pioneering work [38], where the authors studied the noninteracting Fermi gases in 2D traps using semiclassical Boltzmann equations. For harmonic traps, a closed-form expression was obtained, which showed a quantization for arbitrary evolution time, with repeated transitions of the quantization value. In particular, this quantization goes beyond the early-time regime determined by the Fermi-surface topology without the trapping potential. However, it is possible that

such a quantization strictly relies on harmonic traps and details of the experimental protocol, which makes the underlying physics less universal.

In this Letter, we show that it is indeed the opposite: The quantization for arbitrary time $t$ is stable against local continuous deformations of both the trapping potential and experimental details as illustrated in Fig. 1, and which thus defines a variant of the universal topological response in trapped quantum many-body systems. As we will explain, the nonlinear quantized response in $D$-dimensional harmonic traps is a direct consequence of its 1D counterparts. Consequently, we will first state our main conclusion in 1D, with a proposal for the experimental protocol, and then turn to the technique proofs supported by various numerical results. We also discuss practical considerations which are necessary for realistic experiments as in Ref. [38]. Finally, we will explain the generalization to higher dimensions by a tensor product of 1D protocols in each spatial direction. Our theory can be tested in near-term experiments using ultracold atomic gases.

*The statement.* We first present our main result in 1D. Let us consider quantum systems described by the 1D single-particle Hamiltonian

$$\hat{H} = \frac{\hat{p}^2}{2m} + V(\hat{x}), \tag{1}$$

with an asymptotically quadratic trapping potential $V(x) \rightarrow \frac{1}{2}m\omega^2 x^2$ for $|x| \rightarrow \infty$ [39]. For conciseness, we set $m = \omega = 1$ throughout this Letter. We label the single-particle eigenstate of $\hat{H}$ with energy $E_n$ as $|n\rangle$. We consider the experimental protocol sketched in Fig. 1, which is similar to the 2D protocol proposed in Ref. [38]:

(1) The many-body system is prepared into an initial state where the filling fraction of each single-particle state $|n\rangle$ is given by $\langle c_n^\dagger c_n \rangle = f_\Lambda(n)$.

(2) An optical pulse is applied to create a potential [40] $\hat{V}_p = \xi \Theta_p(\hat{x})\delta(t)$ for a half-infinite region. After the pulse, each single-particle state becomes $|\psi_n(0^+)\rangle = e^{-i\xi\Theta_p(\hat{x})}|n\rangle$.
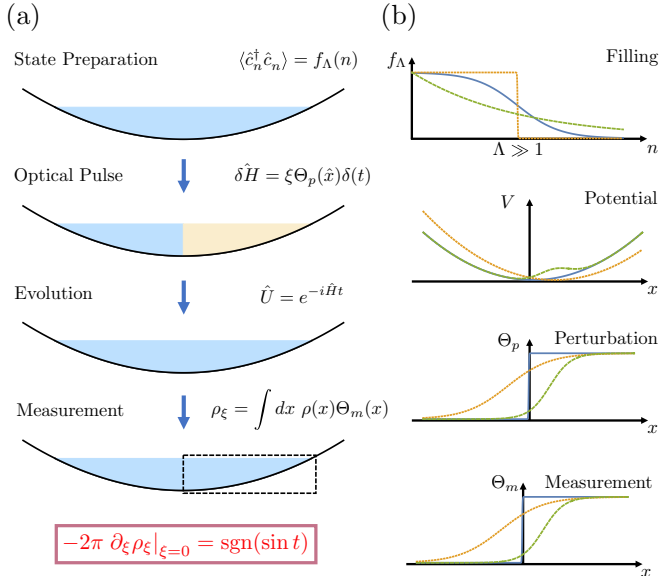
FIG. 1. (a) A sketch of the experimental protocol for the quantized topological response. Details of the protocol are given in the main text. (b) Some examples for local continuous deformations of the atom distribution $f_\Lambda$, trapping frequency $V$, spatial envelope of the optical response $\Theta_p$, and the measurement region $\Theta_m$ under which the universal quantized response is valid. Here, different lines (the blue solid line, the orange dotted line, and the green dashed line) are examples of different functions for which the experimental protocol works.

(3) The density of the system $\rho(x, \xi)$ is measured after the evolution of time $t$. We then analyze the experimental data by computing $\rho_\xi = \int dx\, \rho(x, \xi) \Theta_m(x)$.

(4) We repeat steps 1–3 for different $\xi$ and extract the response at small $\xi$. We then compute $\mathcal{P} \equiv -2\pi\, \partial_\xi \rho_\xi |_{\xi=0}$.

Here, $\hat{U} = e^{-i\hat{H}t}$ is the unitary evolution of single-particle states. We focus on thermodynamical systems satisfying $f_\Lambda(n \ll \Lambda) = 1$ and $f_\Lambda(n \gg \Lambda) = 0$ with $\Lambda \gg 1$, which is naturally realized in noninteracting degenerate Fermi gases with a large number of atoms [41]. The charge response $\mathcal{P}$ can be computed using the linear-response theory. For $\Theta_{m/p}(x)$ that satisfies the boundary condition [see Fig. 1(b)]

$$\Theta_{m/p}(x) = \begin{cases} 1, & x \to \infty, \\ 0, & x \to -\infty, \end{cases} \tag{2}$$

the main conclusion of this Letter reads

$$\mathcal{P} = \lim_{\Lambda \to \infty} 2\pi i \sum_n f_\Lambda(n) \langle n|[\hat{U}^\dagger \Theta_m(\hat{x})\hat{U}, \Theta_p(\hat{x})]|n\rangle$$

$$= \mathrm{sgn}(\sin t). \tag{3}$$

Since the right-hand side of (3) is independent of the details of $(f_\Lambda, V, \Theta_p, \Theta_m)$, the quantized number $\mathcal{P}$ is topological, which means the invariance is under local continuous deformations. In the short-time limit $t \ll 1$, we have $\mathcal{P} = 1$, which probes the topology of the Fermi surface in 1D [27,38]. Intuitively, for harmonic traps $V(x) = x^2/2$, the quantization of the charge response for arbitrary time $t$ can be understood (semiclassically) by noticing that all atoms in the system oscillate with frequency $\omega = 1$ under time evolution. For traps

with local deformations, the quantization is less obvious and is a gift of quantum physics.

Our result is interesting at least for three reasons: First, comparing to previous quantized responses, the trapping potentials play an important role in our setup. The result shows repeated transitions between different quantized values tuned by the evolution time $t$. Second, our response is topological, which means it is invariant under continuous deformations of $(f_\Lambda, V, \Theta_p, \Theta_m)$ with fixed boundary conditions. Third, as discussed later, our result is not restricted to systems in 1D or in thermal equilibrium. It can be generalized to quantum quenches and systems in higher dimensions.

Note that at step 4 we have to repeat the experiment for different $\xi$ to extract the slope $\partial_\xi \rho$. For potentials and measurement envelopes with reflection symmetry $V(-x) = V(x)$ and $\Theta_m(-x) = 1 - \Theta_m(x)$, an alternative protocol exists, which only requires experimental data for a single small $\xi$:

(3′) The density of the system $\rho(x, \xi)$ is measured after the evolution of time $t$. We then compute $\rho_\xi^+ = \int dx\, \rho(x, \xi) \Theta_m(x)$ and $\rho_\xi^- = \int dx\, \rho(x, \xi)[1 - \Theta_m(x)]$.

(4′) In the thermodynamical limit $\Lambda \gg 1$, the statement (3) predicts a quantized response for $\xi \ll 1$:

$$-\pi(\rho_\xi^+ - \rho_\xi^-)/\xi = \mathcal{P} = \mathrm{sgn}(\sin t).$$

Now we turn to the proof of the statement. In the following sections, we prove (3) by first evaluating the left-hand side (LHS) using a particular choice of $(f_\Lambda, V, \Theta_p, \Theta_m)$, and then revealing its topological nature by showing its invariance under local continuous deformations of these functions. Direct numerical verifications will also be presented.

*Explicit calculation.* We first compute (3) in a particular setup with $f_\Lambda(n) = e^{-E_n/\Lambda}$ and $V(x) = \frac{1}{2}x^2$. Introducing $\epsilon = \Lambda^{-1}$, the LHS of (3) becomes

$$\mathcal{P} = 4\pi \lim_{\epsilon \to 0} \mathrm{Im\, tr}[e^{-\epsilon\hat{H}} \Theta_p(\hat{x}) e^{i\hat{H}t} \hat{\Theta}_m(\hat{x}) e^{-i\hat{H}t}]. \tag{4}$$

Here, the trace is over the single-particle Hilbert space. In our choice, the regulator becomes a short imaginary-time evolution, which makes an explicit calculation possible. Using the single-particle Green's function $K(x, y, t) = \langle x|e^{-i\hat{H}t}|y\rangle$, we can write (4) as

$$\mathcal{P} = 4\pi \lim_{\epsilon \to 0} \mathrm{Im} \int dx\, dy\, \Theta_m(x) \Theta_p(y) K(x, y, t - i\epsilon) K(y, x, -t). \tag{5}$$

In harmonic traps, we have a closed-form expression [42] $K(x, y, t) = \frac{1}{\sqrt{2\pi i \sin t}} \exp(\frac{i}{2 \sin t}[(x^2 + y^2) \cos t - 2xy])$. We further choose $\Theta_p(x) = \Theta_m(x) = \theta(x)$. Here, $\theta(x)$ is the unit step function. For $t \neq l\pi$ ($l \in \mathbb{Z}$), we can perform the integral over $x$ and $y$, and expand for small $\epsilon$. Leaving details for the Supplemental Material [43], we find

$$\mathcal{P} = 4\pi \lim_{\epsilon \to 0} \left( \frac{|\sin t|}{4\pi \sin t} + O(\epsilon^2) \right) = \mathrm{sgn}(\sin t). \tag{6}$$

This also indicates the result (3) converges with power-law corrections for a smooth cutoff function $f_\Lambda(n)$. We also need to examine the results at the transition time $t = l\pi$. In this case, the Green's function is proportional to $\delta(x - (-1)^l y)$, which is equivalent to the identity operator $\hat{I}$ or the parity

TABLE I. Numerical results of $\mathcal{P}$ for different choices of $\Theta_m(x)$ and $\Theta_p(x)$. We fix $f_\Lambda(n) = e^{-E_n/\Lambda}$, $V(x) = \frac{1}{2}x^2$, and $\Lambda = 10^4$. The results showed verify our statement (3) to high accuracy, consistent with a quantized value for $\mathcal{P}$. We have also tested the deviation from $\pm 1$ decreases as $\Lambda$ increases.

| | $t = \frac{\pi}{3}$ | $t = \frac{\pi}{2}$ | $t = \frac{3\pi}{2}$ | $t = \frac{7\pi}{4}$ |
|---|---|---|---|---|
| $\Theta_m = \theta(x)$, $\Theta_p = \theta(x)$ | 1.0000 | 1.0000 | $-1.0000$ | $-1.0000$ |
| $\Theta_m = \theta(x+1)$, $\Theta_p = \theta(x+1)$ | 0.9999 | 0.9999 | $-0.9999$ | $-0.9999$ |
| $\Theta_m^{-1} = (e^{-x} + 1)$, $\Theta_p^{-1} = (e^{-x} + 1)$ | 0.9996 | 0.9997 | $-0.9997$ | $-0.9993$ |
| $\Theta_m = \theta(x)$, $\Theta_p = \theta(x+1)$ | 0.9999 | 1.0000 | $-1.0000$ | $-0.9999$ |
| $\Theta_m = \theta(x)$, $\Theta_p^{-1} = (e^{-x} + 1)$ | 0.9998 | 0.9998 | $-0.9998$ | $-0.9997$ |
| $\Theta_m = \theta(x+1)$, $\Theta_p^{-1} = (e^{-x} + 1)$ | 0.9997 | 0.9998 | $-0.9998$ | $-0.9996$ |

operator $\hat{P}$. In either case, $\hat{U}^\dagger \Theta_m(\hat{x})\hat{U}$ is then diagonal in real space, and thus commutes with $\Theta_p(\hat{x})$. This leads to $\mathcal{P} = 0$ for $t = l\pi$.

*Topological invariance.* Having verified (3) for a particular choice of $(f_\Lambda, V, \Theta_p, \Theta_m)$, we now explain its invariance under local continuous deformations. Loosely speaking, the invariance with respect to the deformation of $f_\Lambda$ is a direct consequence of the existence of the limit $\Lambda \to \infty$, which requires the contribution from states $|n\rangle$ to vanish rapidly enough as $n \to \infty$. As a result, for two different choices $f_\Lambda$ and $f'_\Lambda$, their difference is peaked near $n \approx \Lambda$, and thus vanishes as we take $\Lambda \to \infty$. This suggests that $f_\Lambda(n)$ can be viewed as a regulator, whose specific form should not change the underlying physics. More generally, one can take arbitrary initial states in which low-energy Hilbert space is occupied. This includes the thermal equilibrium state with a completely different trapping potential $\tilde{V}(\hat{x})$, where our statement (3) now describes a quantized topological response in the quench dynamics [43].

To understand the invariance of $\mathcal{P}$ for different $(V, \Theta_p, \Theta_m)$, we first imagine the case in which the dimension $d_H$ of the Hilbert space spanned by states $|n\rangle$ is finite. Then, we can safely take the limit of $\lim_{\Lambda \to \infty} f_\Lambda(n) = 1$, and the LHS of (3) becomes $2\pi i \, \mathrm{tr}[\hat{U}^\dagger \Theta_m(\hat{x})\hat{U}, \Theta_p(\hat{x})] = 0$. Here, we have used the cyclic property of the trace operation. As a comparison, our result in (3) is finite for general $t$. The reason is that, without any regulation, both $\mathrm{tr}[\hat{U}^\dagger \Theta_m(\hat{x})\hat{U}\Theta_p(\hat{x})]$ and $\mathrm{tr}[\Theta_p(\hat{x})\hat{U}^\dagger \Theta_m(\hat{x})\hat{U}]$ are divergent [44], and it is not possible to use the cyclic property of the trace. [We avoid possible confusion by introducing an explicit regulator in (3).] This is similar to the derivation of the chiral anomaly [45], and the real-space definition of the 2D Chern number for systems without translation symmetry introduced in Appendix C of Ref. [10]. Interestingly, in the latter case, the formula takes a form that is similar to (3): $(2\pi i)$ times a trace of the commutator between asymptotically projective operators.

Then, let us consider the difference of $\mathcal{P}$ between two different spatial envelopes of the optical impulse $\Theta'_p = \Theta_p + \delta\Theta_p$ and $\Theta_p$:

$$\delta\mathcal{P} = \lim_{\Lambda \to \infty} 2\pi i \sum_n f_\Lambda(n)\langle n|[\hat{U}^\dagger(\Theta_m(\hat{x})-1/2)\hat{U}, \delta\Theta_p(\hat{x})]|n\rangle. \quad (7)$$

Here, we have added a $-1/2$ for later convenience, which trivially commutes with an arbitrary function. When $\delta\Theta_p(x)$ vanishes rapidly enough at $|x| \to \infty$, the limit of $\Lambda \to \infty$ can now be safely taken at first since $\mathrm{tr}[\hat{U}^\dagger(\Theta_m(\hat{x}) - \frac{1}{2})\hat{U}\delta\Theta_p(\hat{x})]$

and $\mathrm{tr}[\delta\Theta_p(\hat{x})\hat{U}^\dagger(\Theta_m(\hat{x}) - \frac{1}{2})\hat{U}]$ are both finite. This leads to

$$\delta\mathcal{P} = 2\pi i \, \mathrm{tr}[\hat{U}^\dagger(\Theta_m(\hat{x}) - 1/2)\hat{U}, \delta\Theta_p(\hat{x})] = 0. \quad (8)$$

This shows that a local continuous deformation of the $\Theta_p$ leaves $\mathcal{P}$ invariant. Noticing (3) is symmetric under $\Theta_m \leftrightarrow \Theta_p$ and $\hat{U} \to \hat{U}^\dagger$, we conclude that $\mathcal{P}$ is also invariant under the local continuous deformation of the $\Theta_m$. For the deformation of $V$, we can use

$$\delta\hat{U}(t) = -i \int_0^t dt' \, \hat{U}(t-t')\delta V(\hat{x})\hat{U}(t'). \quad (9)$$

Similar to previous cases, the variation of $\mathcal{P}$ again vanishes when $\delta\hat{V}(x)$ decays rapidly enough at $|x| \to \infty$.

Now we present numerical verification of the topological invariance for different choices of $(f_\Lambda, V, \Theta_p, \Theta_m)$. The details of the numerics can be found in the Supplemental Material [43]. We first fix $f_\Lambda(n) = e^{-\epsilon E_n}$ and $V(x) = \frac{1}{2}x^2$. The quantization of the response $\mathcal{P}$ can then be tested to high accuracy by performing the numerical integration in (5) with small $\epsilon = 10^{-4}$. The result is presented in Table I, which is consistent with the statement (3). We then test the validity of the statement for different choices of the cutoff function $f_\Lambda(n)$ and potential $V(x)$ with fixed $\Theta_m(x) = \Theta_p(x) = \theta(x)$. Since generally no closed-form expression is available for the Green's function $K(x, y, t)$, we perform an exact diagonalization study in the Hilbert space spanned by the first $L = 200$ eigenstates of the harmonic oscillator. Leaving details for the Supplemental Material [43], we present results in Fig. 2 for $\Lambda = 150$. Despite a finite $\Lambda$, the results match the statement (3) to good accuracy. This guarantees the quantization can be observed in experiments with a moderate number of atoms.

*Practical considerations.* In realistic experiments the duration of the optical pulse is finite. To estimate the corresponding effect, we make the replacement

$$\hat{V}_p = \xi\Theta_p(\hat{x})\delta(t) \to \frac{\xi}{\sqrt{2\pi\sigma^2}}\Theta_p(\hat{x})e^{-\frac{t^2}{2\sigma^2}}.$$

Using the linear-response theory, we can determine the density change due to the optical pulse as

$$\mathcal{P}_\sigma \equiv -2\pi \, \partial_\xi \rho_\xi(t)|_{\xi=0} = \int dt' \frac{1}{\sqrt{2\pi\sigma^2}}e^{-\frac{t^2}{2\sigma^2}}\mathcal{P}(t-t'). \quad (10)$$

For a short duration of the pulse $\sigma\omega \ll 1$, $\mathcal{P}_\sigma$ is approximately quantized for $|t - n\pi| \gtrsim \sigma$. The correction of finite $\sigma$ is important near the transition time $t \approx n\pi$. In this case,
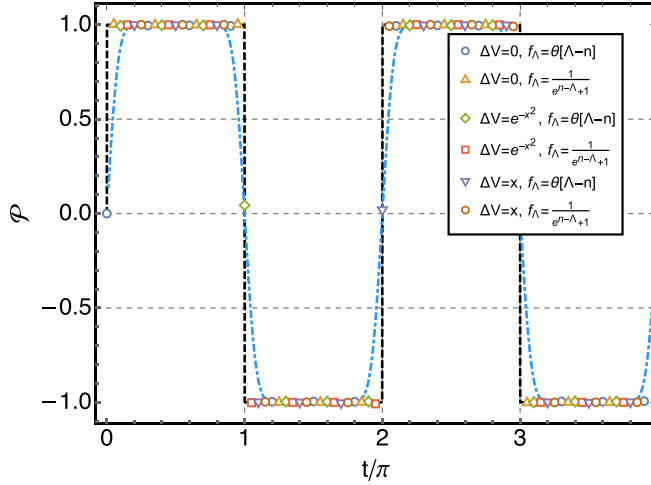
FIG. 2. The numerical results of $\mathcal{P}$ for different potential $V(x) = [x^2 + \Delta V(x)]/2$ and filling fraction $f_\Lambda(n)$ with finite $\Lambda = 150$. The black dashed line is the quantized analytical prediction (3). The results show deviations of the order of $\sim 10^{-2}$, which is consistent with the quantization of $\mathcal{P}$. The blue dotted-dashed line is a plot of (11), which estimates the effects of finite duration of the optical pulse in realistic experiments. Here, we set $\sigma = 0.2$.

we can estimate the correction by approximating $\mathcal{P}(t) \approx (-1)^n \operatorname{sgn}(t - n\pi)$, which gives

$$\mathcal{P}_\sigma \approx (-1)^n \operatorname{erf}\left(\frac{t - \pi n}{\sqrt{2}\sigma}\right), \quad \text{for } |t - \pi n| \lesssim \sigma. \quad (11)$$

This describes the smoothening of the response function near $t \approx \pi n$. A plot of (11) with $\sigma = 0.2$ is presented using the blue dotted-dashed line in Fig. 2. For $|t - n\pi| \gtrsim \sigma$, it converges to the quantized value with exponentially small corrections. This suggests the quantized response (3) is stable against a finite duration of the optical pulse.

On the other hand, there are also residual interactions between atoms in realistic experiments. We estimate the contribution from off-resonant interactions for 1D Fermi gases. Because of the Fermi statistics, the odd-wave interaction, an analog of the $p$-wave interaction in higher dimensions, dominates at low temperatures $\hat{H}_I = g \int dx (\hat{\psi}^\dagger \partial_x \hat{\psi}^\dagger)(\hat{\psi} \partial_x \hat{\psi})$. Away from any two-body resonance, $g$ can be estimated by the van der Waals length $l_W$ [46], which is usually hundreds of picometers $\sim 10^{-10}$ m. On the other hand, the typical trapping frequency $\omega$ is $\sim 50$ Hz in most cold-atom experiments, which is equivalent to a typical length $l_h \sim 10^{-5}$ m. Consequently, we expect the effect of the interaction, estimated by $N l_W / l_h \ll 1$, can be neglected for a moderate number of atoms.

*Higher dimensions.* Finally, we study the implication of our statement (3) in $D$-dimensional harmonic traps. The Hamiltonian reads

$$H = \sum_{a=1}^{D} H_a = \sum_{a=1}^{D} \left(\frac{\hat{p}_a^2}{2} + \frac{\hat{x}_a^2}{2}\right). \quad (12)$$

Here, we have assumed the trapping frequency $\omega_a = 1$. Generalizations to anisotropic harmonic traps are straightforward. We propose the following protocol to probe the nonlinear

response of trapped quantum gases, as an analog of the quantized nonlinear conductance in ballistic metals [27]: After preparing the initial state, we add an optical pulse with

$$\hat{V}_p = \sum_a \xi_a \Theta_p^a(\hat{x}) \delta\left(t - t_a^0\right). \quad (13)$$

We have set $t_1^0 = 0$ in the previous discussions for the 1D protocol. We then let the system evolve to time $t$, and perform the measurement of $\prod_a \Theta_m^a(\hat{x}_a)$ to obtain $\rho_{\{\xi\}} \equiv \langle \prod_a \Theta_m^a(\hat{x}_a) \rangle$. Both $\Theta_m^a$ and $\Theta_p^a$ satisfy the same boundary condition as their 1D counterparts. Taking the response in each direction to the linear order, we define the nonlinear charge response $\mathcal{P}^{(D)}$ as

$$\mathcal{P}^{(D)} = (-2\pi)^D \partial_{\xi_1} \partial_{\xi_2} \cdots \partial_{\xi_D} \rho_{\{\xi\}}|_{\xi_a = 0}. \quad (14)$$

Since the $D$-dimensional harmonic trap is exactly analogous to $D$ copies of independent 1D harmonic traps, the contribution from different $a$ factorizes. Our 1D result (3) implies

$$\mathcal{P}^{(D)} = (2\pi i)^D \lim_{\Lambda \to \infty} \sum_{\{n_a\}} f_\Lambda \prod_{a=1}^{D} \langle [\hat{U}_a^\dagger \Theta_m^a(\hat{x}_a) \hat{U}_a, \Theta_p^a(\hat{x}_a)] \rangle_{n_a}$$

$$= \operatorname{sgn}\left(\prod_a \sin\left(t - t_a^0\right)\right), \quad (15)$$

where $\hat{U}_a = e^{-i\hat{H}_a(t - t_a^0)}$, and $n_a$ is the quantum number in the $x_a$ direction. We have introduced the filling fraction $f_\Lambda(\{n_a\})$, which decays rapidly enough for any $n_a \gg \Lambda$. When $f_\Lambda(\{n_a\}) = \prod_a f_\Lambda(n_a)$, (15) is just $D$ copies of the 1D result (3). We then use the insensitivity of the regulator in the limit of $\Lambda \to \infty$ to relax the restriction of $f_\Lambda(\{n_a\})$. Numerical verifications are presented in the Supplemental Material [43]. When we choose $f_\Lambda(\{n_a\}) = (e^{\beta(\sum_a n_a - \Lambda)} + 1)^{-1}$, the initial state describes a thermal ensemble in $D$ dimensions. For $D = 2$, our protocol is reduced to the protocol proposed in Ref. [38], and our result is consistent with the semiclassical approach with $\theta_p^a = \theta_m^a = \theta(x)$ [38]. Moreover, our analysis in 1D suggests that nonlinear responses in higher dimensions are also topological, regardless of the choices of $(\Theta_p^a, \Theta_m^a)$.

*Discussion.* In this Letter, we introduce a universal quantized charge transport of trapped quantum gases. We compute the response function explicitly for a convenient choice of the setup, and show the result is topologically invariant under local continuous deformations with fixed boundary conditions for the trapping potential $V$, the atom distribution $f_\Lambda$, the spatial envelope of the optical pulse $\Theta_p$, and the measurement region $\Theta_m$. The statement is supported by various numerical results, which match the analytical prediction to high accuracy. After analyzing realistic effects in experiments, we believe our statement (3), as well as its higher-dimensional generalization (15) for nonlinear responses, can be directly observed in near-term experiments using ultracold atomic gases. There are also various interesting future directions, including adding symmetry constraints, considering the effects of thermal baths, and detailed studies of interaction effects.

[1] L. D. Landau and E. M. Lifshitz, *Statistical Physics* (Elsevier, Amsterdam, 2013), Vol. 5.

[2] M. Z. Hasan and C. L. Kane, Rev. Mod. Phys. **82**, 3045 (2010).

[3] X.-L. Qi and S.-C. Zhang, Rev. Mod. Phys. **83**, 1057 (2011).

[4] B. A. Bernevig, in *Topological Insulators and Topological Superconductors* (Princeton University Press, Princeton, NJ, 2013).

[5] E. Witten, Riv. Nuovo Cimento **39**, 313 (2016).

[6] X.-G. Wen, Rev. Mod. Phys. **89**, 041004 (2017).

[7] N. P. Armitage, E. J. Mele, and A. Vishwanath, Rev. Mod. Phys. **90**, 015001 (2018).

[8] R. Moessner and J. E. Moore, *Topological Phases of Matter* (Cambridge University Press, Cambridge, UK, 2021).

[9] B. Zeng, X. Chen, D.-L. Zhou, X.-G. Wen *et al.*, *Quantum Information Meets Quantum Matter* (Springer, Berlin, 2019).

[10] A. Kitaev, Ann. Phys. **321**, 2 (2006).

[11] A. Bansil, H. Lin, and T. Das, Rev. Mod. Phys. **88**, 021004 (2016).

[12] N. Goldman, J. C. Budich, and P. Zoller, Nat. Phys. **12**, 639 (2016).

[13] K. v. Klitzing, G. Dorda, and M. Pepper, Phys. Rev. Lett. **45**, 494 (1980).

[14] Y. K. Kato, R. C. Myers, A. C. Gossard, and D. D. Awschalom, Science **306**, 1910 (2004).

[15] C.-Z. Chang, J. Zhang, X. Feng, J. Shen, Z. Zhang, M. Guo, K. Li, Y. Ou, P. Wei, L.-L. Wang, Z.-Q. Ji, Y. Feng, S. Ji, X. Chen, J. Jia, X. Dai, Z. Fang, S.-C. Zhang, K. He, Y. Wang *et al.*, Science **340**, 167 (2013).

[16] G. Jotzu, M. Messer, R. Desbuquois, M. Lebrat, T. Uehlinger, D. Greif, and T. Esslinger, Nature (London) **515**, 237 (2014).

[17] M. Tarnowski, F. N. Ünal, N. Fläschner, B. S. Rem, A. Eckardt, K. Sengstock, and C. Weitenberg, Nat. Commun. **10**, 1728 (2019).

[18] W. Sun, C.-R. Yi, B.-Z. Wang, W.-W. Zhang, B. C. Sanders, X.-T. Xu, Z.-Y. Wang, J. Schmiedmayer, Y. Deng, X.-J. Liu, S. Chen, and J.-W. Pan, Phys. Rev. Lett. **121**, 250403 (2018).

[19] S. Nakajima, T. Tomita, S. Taie, T. Ichinose, H. Ozawa, L. Wang, M. Troyer, and Y. Takahashi, Nat. Phys. **12**, 296 (2016).

[20] M. Aidelsburger, M. Lohse, C. Schweizer, M. Atala, J. T. Barreiro, S. Nascimbène, N. Cooper, I. Bloch, and N. Goldman, Nat. Phys. **11**, 162 (2015).

[21] M. Atala, M. Aidelsburger, M. Lohse, J. T. Barreiro, B. Paredes, and I. Bloch, Nat. Phys. **10**, 588 (2014).

[22] D. J. Thouless, M. Kohmoto, M. P. Nightingale, and M. den Nijs, Phys. Rev. Lett. **49**, 405 (1982).

[23] F. D. M. Haldane, Phys. Rev. Lett. **93**, 206602 (2004).

[24] C. L. Kane and E. J. Mele, Phys. Rev. Lett. **95**, 146802 (2005).

[25] B. A. Bernevig and S.-C. Zhang, Phys. Rev. Lett. **96**, 106802 (2006).

[26] M. König, S. Wiedmann, C. Brüne, A. Roth, H. Buhmann, L. W. Molenkamp, X.-L. Qi, and S.-C. Zhang, Science **318**, 766 (2007).

[27] C. L. Kane, Phys. Rev. Lett. **128**, 076801 (2022).

[28] R. Landauer, J. Math. Phys. **37**, 5259 (1996).

[29] D. S. Fisher and P. A. Lee, Phys. Rev. B **23**, 6851 (1981).

[30] D. A. Wharam, T. J. Thornton, R. Newbury, M. Pepper, H. Ahmed, J. E. F. Frost, D. G. Hasko, D. C. Peacock, D. A. Ritchie, and G. A. C. Jones, J. Phys. C **21**, L209 (1988).

[31] T. Honda, S. Tarucha, T. Saku, and Y. Tokura, Jpn. J. Appl. Phys. **34**, L72 (1995).

[32] I. van Weperen, S. R. Plissard, E. P. Bakkers, S. M. Frolov, and L. P. Kouwenhoven, Nano Lett. **13**, 387 (2013).

[33] S. Frank, P. Poncharal, Z. L. Wang, and W. A. de Heer, Science **280**, 1744 (1998).

[34] S. Krinner, D. Stadler, D. Husmann, J.-P. Brantut, and T. Esslinger, Nature (London) **517**, 64 (2015).

[35] S. Krinner, T. Esslinger, and J.-P. Brantut, J. Phys.: Condens. Matter **29**, 343003 (2017).

[36] M. Lebrat, S. Häusler, P. Fabritius, D. Husmann, L. Corman, and T. Esslinger, Phys. Rev. Lett. **123**, 193605 (2019).

[37] P. M. Tam, M. Claassen, and C. L. Kane, Phys. Rev. X **12**, 031022 (2022).

[38] F. Yang and H. Zhai, Quantum **6**, 857 (2022).

[39] In realistic experiments, the trapping potential always deviates from being perfectly harmonic at an energy scale $E_0$. Then, we should require that $E_0 \gg \Lambda \gg 1$.

[40] H. Zhai, *Ultracold Atomic Physics* (Cambridge University Press, Cambridge, UK, 2021).

[41] Nevertheless, there is no fundamental distinction between bosons and fermions in 1D. In particular, for interacting bosons in the tonk limit, the many-body wave function in real space matches that of noninteracting fermions up to phases. As a result, the density-density correlator would be the same.

[42] A. Altland and B. D. Simons, *Condensed Matter Field Theory* (Cambridge University Press, Cambridge, UK, 2010).

[43] See Supplemental Material at http://link.aps.org/supplemental/10.1103/PhysRevA.107.L031305 for (1) the derivation of Eq. (6), (2) the numerical details, (3) the numerical verification of the quantized response in quantum quenches, (4) the numerical verification in 2D, and (5) the effect of weak interactions.

[44] As an example, (5) diverges if we set $\epsilon = 0$ at the beginning.

[45] M. Srednicki, *Quantum Field Theory* (Cambridge University Press, Cambridge, UK, 2007).

[46] C. Chin, R. Grimm, P. Julienne, and E. Tiesinga, Rev. Mod. Phys. **82**, 1225 (2010).